# Peroxisome elongation and constriction but not fission can occur independently of dynamin-like protein 1

**Annett Koch[1], Gabriele Schneider[1], Georg H. Lüers[2] and Michael Schrader[1,*]**

[1]Department of Cell Biology and Cell Pathology, Robert Koch Strasse 6, and [2]Department of Anatomy and Cell Biology, Robert Koch Strasse 8, University of Marburg, Marburg, 35037, Germany

*Author for correspondence (e-mail: schrader@mailer.uni-marburg.de)

*Accepted 14 April 2004*
*Journal of Cell Science 117, 3995-4006 Published by The Company of Biologists 2004*
*doi:10.1242/jcs.01268*

## Summary

**The mammalian dynamin-like protein DLP1 belongs to the dynamin family of large GTPases, which have been implicated in tubulation and fission events of cellular membranes. We have previously shown that the expression of a dominant-negative DLP1 mutant deficient in GTP hydrolysis (K38A) inhibited peroxisomal division in mammalian cells. In this study, we conducted RNA interference experiments to 'knock down' the expression of DLP1 in COS-7 cells stably expressing a GFP construct bearing the C-terminal peroxisomal targeting signal 1. The peroxisomes in DLP1-silenced cells were highly elongated with a segmented morphology. Ultrastructural and quantitative studies confirmed that the tubular peroxisomes induced by DLP1-silencing retained the ability to constrict their membranes but were not able to divide into spherical organelles. Co-transfection of DLP1 siRNA with Pex11pβ, a peroxisomal membrane protein involved in peroxisome proliferation, induced further elongation and network formation of the peroxisomal compartment. Time-lapse microscopy of living cells silenced for DLP1 revealed that the elongated peroxisomes moved in a microtubule-dependent manner and emanated tubular projections. DLP1-silencing in COS-7 cells also resulted in a pronounced elongation of mitochondria, and in more dispersed, elongated Golgi structures, whereas morphological changes of the rER, lysosomes and the cytoskeleton were not detected. These observations clearly demonstrate that DLP1 acts on multiple membranous organelles. They further indicate that peroxisomal elongation, constriction and fission require distinct sets of proteins, and that the dynamin-like protein DLP1 functions primarily in the latter process.**

Key words: Peroxisome biogenesis, Dynamin, Organelle division, Peroxisomal membrane protein, Pex11p

## Introduction

Peroxisomes are ubiquitous eucaryotic organelles that contribute to important metabolic processes, including hydrogen peroxide metabolism, the β-oxidation of fatty acids and the biosynthesis of ether lipids (van den Bosch et al., 1992). An interesting feature is their ability to proliferate and multiply, or be degraded in response to nutritional and environmental stimuli. The prevailing model of peroxisome biogenesis, proposed by Lazarow and Fujiki (Lazarow and Fujiki, 1985), predicts that peroxisomes grow by uptake of newly synthesized proteins from the cytosol and multiply by division. A key question in the field is, whether this is the predominant mechanism of peroxisome formation, or are there alternative modes of peroxisome formation which may involve the ER or other kinds of endomembranes (South and Gould, 1999; Titorenko and Rachubinski, 2001; Faber et al., 2002; Geuze et al., 2003).

At present, little is known about the proteins required for growth and division of the peroxisomal compartment. The peroxisomal membrane protein Pex11p has been proposed to function in peroxisome division in a variety of species (Erdmann and Blobel, 1995; Marshall et al., 1995; Sakai et al., 1995; Passreiter et al., 1998; Schrader et al., 1998b; Lorenz et al., 1998). Overexpression of Pex11p promotes peroxisome elongation and subsequent division, whereas loss of Pex11p results in reduced peroxisome number (Erdmann and Blobel, 1995; Marshall et al., 1995; Schrader et al., 1998b; Li et al., 2002). A striking increase in elongated forms of peroxisomes upon expression of Pex11p has been observed in all organisms studied, indicating that tubule formation may be an important aspect of peroxisome division (Schrader et al., 1996; Schrader et al., 1998b). Mammalian cells express at least three distinct Pex11 genes (Pex11pα, β, γ), whereas *Saccharomyces cerevisiae* has a single Pex11 gene (Li et al., 2002). However, recent findings indicate that Pex25p and the novel peroxin Pex27p are Pex11p-related proteins, which are involved in the regulation of peroxisome size and number in *S. cerevisiae* (Smith et al., 2002; Rottensteiner et al., 2003; Tam et al., 2003). The biochemical properties of Pex11p are still a matter of debate and there is currently no mechanistic model for peroxisome division. Evidence for a metabolic control of peroxisome division has also been presented (Poll-The et al., 1988; Sacksteder and Gould, 2000; Smith et al., 2002) and might be mediated by signals derived from the β-oxidation of fatty acids (Chang et al., 1999; van Roermund et al., 2000). However, Pex11p can induce peroxisome proliferation

independently of peroxisome metabolism (Li and Gould, 2002).

Other proteins involved in peroxisome division are members of the dynamin family of large GTPases, which have been implicated in tubulation and fission events of cellular membranes (McNiven, 1998; Danino and Hinshaw, 2001). The dynamin-related protein Vps1p mediates peroxisome division in *S. cerevisiae* (Hoepfner et al., 2001), whereas the dynamin-like protein DLP1 has recently been shown to be required for peroxisomal fission in mammalian cells (Koch et al., 2003; Li and Gould, 2003). Mammalian DLP1 and its homologues Dnm1 (*S. cerevisiae*) and DRP-1 (*C. elegans*) are also suggested to be involved in the control of mitochondrial morphology and division (Yoon et al., 1998; Labrousse et al., 1999; Smirnova et al., 2001). We have recently shown that the expression of a dominant-negative DLP1 mutant deficient in GTP hydrolysis (K38A) inhibited peroxisomal division in mammalian cells (Koch et al., 2003). In this study, we have performed RNA interference experiments which were combined with protein expression, ultrastructural and live cell studies, to examine the effects of reduced DLP1 protein levels on peroxisome morphology and division as well as on other intracellular organelles in more detail.

## Materials and Methods

### cDNAs and antibodies

Plasmid pVgRXR was obtained from Invitrogen (Groningen, The Netherlands) and plasmid pGHL97, for expression of a fusion protein of the green fluorescent protein with a peroxisomal targeting signal (GFP-PTS1), was described earlier (Luers et al., 2003). Wild-type DLP1 (DLP1-WT) and DLP1 fused to GFP (DLP1-WT-GFP) were described previously (Pitts et al., 1999). The C-terminally tagged version of Pex11pβmyc in pcDNA3 was described by Schrader et al. (Schrader et al., 1998b). MBGV-GP, encoding the glycoprotein GP of the Marburg virus, as well as MBGV-GP-specific polyclonal antibodies were kindly provided by Dr S. Becker (University of Marburg, Germany) (Becker et al., 1996). Rabbit polyclonal anti-PMP70 (peroxisomal membrane protein 70) antibodies (Luers et al., 1993) were a gift from Dr A. Völkl (University of Heidelberg, Germany). The rabbit polyclonal anti-DLP1 antibody was described previously (Yoon et al., 1998). The following monoclonal antibodies were used: anti-p115 (Transduction Laboratories); anti-myc epitope 9E10 (kindly provided by Dr M. Eilers, University of Marburg, Germany); anti-MnSOD MnS-1 (mangan superoxide dismutase) (Alexis Corporation, San Diego, CA, USA), anti-tubulin DM1α (Sigma). Species-specific anti-IgG antibodies conjugated to TRITC or FITC were obtained from Dianova (Hamburg, Germany).

### Cell culture

COS-7 cells stably expressing GFP-PTS1 were generated by electroporation using the Easyject Optima electroporation system (Peqlab, Erlangen, Germany), and were transfected with a mixture of 2 μg of plasmid pVgRXR with 10 μg of plasmid pGHL97. Transfected cells were selected in medium supplemented with 0.1 mg/ml of Zeocin (Invitrogen) for 10 days. Surviving cell clones were analyzed by fluorescence microscopy for expression of the GFP-PTS1 fusion protein and positive clones were isolated for further analysis. One of the resulting cell clones with homogeneous expression of the GFP-PTS1, named BGL211, was used for this study. Cells were cultured in Dulbecco's modified Eagle's medium (DMEM) supplemented with 2 g/l sodium bicarbonate, 2 mM glutamine, 100 U/ml penicillin, 100 μg/ml streptomycin and 10% fetal calf serum (all from PAA Laboratories GmbH, Germany) at 37°C in a humidified atmosphere containing 5% $CO_2$. HepG2 cells were cultured under the same conditions.

### RNA interference and transfection experiments

To knock down the expression of DLP1 by RNA interference, 21-nucleotide RNAs were obtained from Dharmacon (Lafayette, CO, USA) and annealed according to the manufacturer's instructions. The siRNA sequence efficiently targeting human DLP1 (accession no. NM012062) corresponded to the coding region 783-803 relative to the first nucleotide of the start codon (siRNA D1, sense strand: 5′-UCCGUGAUGAGUAUGCUUUdTdT-3′). A second siRNA sequence (siRNA D2, sense strand: 5′-UUACCUUCAGCUGUA-UCACdTdT-3′) turned out to be less efficient in silencing DLP1. Transfection of siRNA was carried out using Oligofectamine (Invitrogen) according to the manufacturer's instructions. As a control, cells were either transfected with buffer or with siRNA duplexes targeting luciferase (Dharmacon). Cells were usually transfected with siRNA duplexes or buffer 24 and 48 hours after seeding and assayed for silencing and organelle morphology 72 hours after seeding by immunofluorescence and immunoblotting. Cells were treated 48 hours after the first transfection with siRNA duplexes with 10 μM nocodazole for 2-12 hours at 37°C. Silenced cells and controls were transfected with DNA constructs 48 hours after seeding by incubation with polyethylenimine (25 kDa PEI, Sigma) as described previously (Fischer et al., 1999). Transfection of COS-7 cells with a DLP1-WT or DLP1-WT-GFP construct was performed by electroporation (Schrader et al., 1998b). Cells were afterwards seeded at a defined density of $2\times10^5$ cells/ml and processed for immunofluorescence after 24 and 48 hours when tubular peroxisomes reached their maximum (Schrader et al., 1996).

### Indirect immunofluorescence

Cells grown on glass coverslips were fixed with 4% paraformaldehyde in PBS, pH 7.4, permeabilized with 0.2% Triton X-100 or 25 μg/ml digitonin and incubated with primary and secondary antibodies as described (Schrader et al., 1996). Silenced cells were usually processed for immunofluorescence 48-72 hours after the first transfection with siRNA duplexes. Samples were examined using a Leitz Diaplan (Leica, Wetzlar, Germany) or an Olympus BX-61 microscope (Olympus Optical Co. GmbH, Hamburg, Germany) equipped with the appropriate filter combinations and photographed on Kodak TMY film or digitalized using a F-view II CCD camera (Soft Imaging System GmbH, Münster, Germany). Digital images were optimized for contrast and brightness using Adobe Photoshop software.

### Live cell imaging

Cells were grown in culture dishes with a glass bottom. For time-lapse studies they were placed in a temperature and $CO_2$ controlled chamber (Carl Zeiss; CTI Controller 3700, TRZ 3700) on a heating stage of a Zeiss LSM 410 inverted microscope (Carl Zeiss) equipped with a ×63/1.4 objective. As a light source, an argon ion laser, of wavelength 488 nm with appropriate filter combinations was used. Images were collected at 5 second intervals for up to 5 minutes, and the cells were monitored at various times for a total of 1-4 hours. Cells were treated with 33 μM nocodazole by adding the microtubule-destabilizing agent directly to the live cell imaging assay and incubating for 15-30 minutes.

### Electron microscopy

Cells were fixed in 0.2 M sodium phosphate buffer, pH 7.4, containing 4% paraformaldehyde, 0.05% glutaraldehyde (Serva, Heidelberg,

Germany) and 2% sucrose. For cytochemical localization of catalase (Angermuller and Fahimi, 1981), the cells were incubated in alkaline DAB medium followed by postfixation in 1% aqueous osmium tetroxide and 2% uranyl acetate. The samples were dehydrated in a graded series of alcohol and embedded in Epon 812 (Polysciences Ltd., Eppenheim, Germany). Sections were stained with lead citrate and examined with a Zeiss EM 9S electron microscope.

### Isolation of peroxisomes

Peroxisomes were isolated according to a protocol described previously (Völkl et al., 1996) with slight modifications. Briefly, COS-7 cells were homogenized with a Potter S homogenizer (Braun, Melsungen, Germany; 1 stroke, 2 minutes, 1000 rpm) in ice-cold homogenization buffer (250 mM sucrose, 5 mM Mops, 0.1% ethanol, 1 mM EDTA, 0.2 mM PMSF, 1 mM 6-aminocaproic acid, 5 mM benzamidine, 10 μg/ml leupeptin, 0.2 mM DTT, pH 7.4). The homogenate was subfractionated by differential pelleting, employing several centrifugation steps at 50 ***g*** and 2860 ***g***, yielding a supernatant, which was layered onto two Nycodenz (Nycomed Pharma, Oslo, Norway) cushions: 65% Nycodenz (ρ=1.346 g/ml) and 32.5% Nycodenz (ρ=1.172 g/ml), in homogenization buffer without sucrose. After centrifugation at 37500 ***g*** in a Beckman L5-65B ultracentrifuge (Beckman Instruments, Munich, Germany; 45 Ti rotor, 4°C, 30 minutes), the peroxisomal fraction, banding at the phase border of the two Nycodenz cushions, was obtained.

### Gel electrophoresis and immunoblotting

Protein samples were separated by SDS-PAGE, transferred to nitrocellulose (Schleicher and Schüll, Dassel, Germany) using a semi-dry apparatus and analyzed by immunoblotting. Immunoblots were processed using HRP-conjugated secondary antibodies and enhanced chemiluminescence reagents (Amersham Corp., Arlington Heights, LL, USA). For quantification, immunoblots were scanned and processed using Pcbas software.

### Quantitation and statistical analysis of data

For quantitative evaluation of organelle morphology, 100-200 cells per coverslip were examined and categorized accordingly. Usually, four coverslips per preparation were analyzed, and three to seven independent experiments were performed. Significant differences between experimental groups were detected by analysis of variance for unpaired variables using Microsoft Excel. Data are presented as means ± s.d., with an unpaired *t*-test used to determine statistical differences. *P* values <0.05 are considered as significant, and *P* values <0.01 are considered as highly significant.

## Results

### Silencing of DLP1 induces elongation of peroxisomes

In a recent study we provided evidence that the dynamin-like GTPase DLP1 is involved in peroxisomal fission in mammalian cells (Koch et al., 2003). Most of our studies have been performed by expressing a dominant-negative DLP1 mutant in combination with the peroxisomal membrane protein Pex11pβ. By this approach we took advantage of an earlier observation that overexpression of Pex11pβ induces peroxisome proliferation and division (Schrader et al., 1998b). Now, we conducted RNA interference experiments to study the effects of reduced DLP1 mRNA and DLP1 protein levels on peroxisome morphology and division in more detail. DLP1 siRNA duplexes specific for human DLP1 were designed according to the method of Elbashir et al. (Elbashir et al., 2001). For our studies, we selected a duplex (D1) that targeted a conserved region, which is found in multiple isoforms of DLP1 that are generated by alternative splicing of the initial DLP1 transcript (McNiven et al., 2000). The encoded amino acids are conserved among different species and have also been used to generate specific antibodies to DLP1 (Yoon et al., 1998). Another duplex (D2) targeting a region in the 5′ region of human DLP1 turned out to be less effective (not shown).

The duplex (D1) was transfected into COS-7 cells stably expressing a GFP construct bearing the C-terminal peroxisomal targeting signal 1 (GFP-PTS1). Cells were usually processed for immunoblot and immunofluorescence analyses 48 hours after transfection (72 hours in culture) using antibodies directed to DLP1. Immunoblots of cell homogenates demonstrated that the DLP1 protein level was reduced to 30-35% of the control level (Fig. 1G). Since the transfection efficiency is usually about 70-80%, the DLP1 protein level is even lower in those cells that took up the DLP1 siRNA (see Fig. 3). A significant reduction in DLP1 protein level was not observed in controls either treated with buffer or transfected with a luciferase siRNA duplex. The immunoblot results were confirmed by immunofluorescence studies. DLP1 was barely detectable in silenced cells, whereas in controls a fine, punctate cytoplasmic staining pattern for DLP1 was observed (Fig. 1B,D and Fig. 3A,B). The GFP-labeled peroxisomes in the majority of the control cells had a spherical appearance (buffer treatment: 95±4.4%; luciferase siRNA: 93±1.6%, 48 hours after transfection). In contrast, there was a drastic change in peroxisomal morphology in DLP1-silenced cells. Approximately 70-80% of the cell population exhibited peroxisomes with a highly elongated, tubular morphology (Fig. 1C,E-F and Fig. 3A,B). Tubules measuring 5 μm up to 15 μm in length were frequently observed. Interestingly, nearly all elongated, tubular peroxisomes induced by DLP1 silencing had a segmented appearance (95% of the cells exhibiting tubular peroxisomes) (Fig. 1C,E and Fig. 3A,B). A segmentation was also observed with antibodies directed to peroxisomal matrix proteins (catalase, acyl-CoA oxidase) or to PMP70, a peroxisomal membrane protein (not shown). However, the elongated, segmented peroxisomes were not observed to separate into spherical organelles when quantified after different time intervals after transfection (Fig. 1F). Since the sequence targeted by duplex D1 is conserved, we have investigated the effect of DLP1-silencing on the peroxisomal compartment in cells from different species. Similar morphological changes of peroxisomes than the ones described above were obtained with a variety of other cell lines of human (HepG2, HeLa) or rodent origin (Fao, AR42J) (not shown). However, differences in the transfection efficiency, the level of DLP1 reduction and in the length of tubular peroxisomes were observed. The alterations of peroxisome morphology could be best studied in COS-7 and HepG2 cells, with COS-7 cells exhibiting the most elongated peroxisomal tubules. The peroxisomal phenotypic changes found in these and other cells are consistent with a direct function of mammalian DLP1 in peroxisomal fission.

### DLP1 is not directly involved in peroxisomal constriction

To examine peroxisomal morphology at the ultrastructural level, we performed electron microscopy of DLP1-silenced

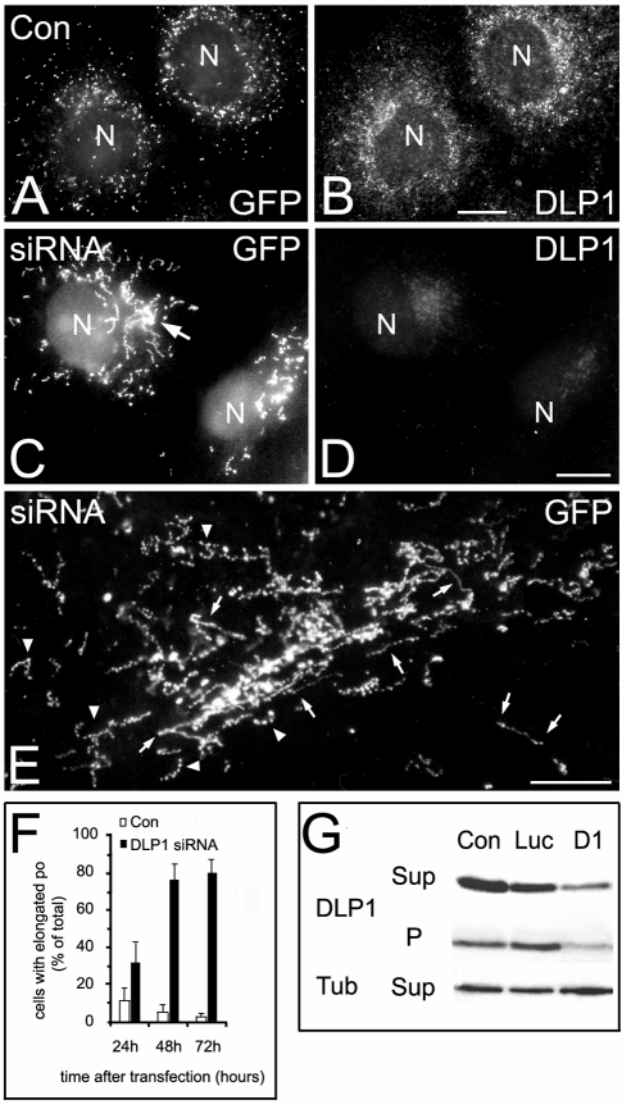


**Fig. 1.** Silencing of DLP1 induces elongation of the peroxisomal compartment. COS-7 cells stably expressing GFP-PTS1 were transfected with DLP1 siRNA duplexes (siRNA) and processed for immunofluorescence (A-E) and immunoblotting (G) with anti-DLP1 antibodies 48 hours after the first transfection. (A,B) Control cells (Con) transfected with luciferase siRNA duplexes. (C-E) COS-7 cells transfected with DLP1 siRNA duplexes. The arrow in C points to a peroxisomal aggregate. (E) A high magnification view of elongated peroxisomes. Note the segmented appearance of the organelles (arrowheads). Arrows point to largely elongated, tubular peroxisomes. N, nucleus. (F) Quantification of peroxisome morphology at different time points after transfection with siRNA. The data are from five to seven independent experiments and are expressed as means ± s.d. ($P$<0.01 when compared to controls). (G) Immunoblots of homogenates prepared from controls treated with buffer (Con) and cells transfected with luciferase (Luc) or DLP1 siRNA duplexes (D1) using anti-DLP1 and anti-tubulin (Tub) antibodies. Homogenates were separated in a supernatant (Sup) and pellet (P) fraction. Equal amounts of protein (DLP1, 70 μg/lane; Tub, 30 μg/lane) were loaded onto the gels. Anti-tubulin was used to check for equal loading and integrity of the cells after transfection. Bars, 10 μm.

cells. To achieve a specific and prominent labeling of peroxisomes, we used the alkaline DAB reaction for catalase (Angermuller and Fahimi, 1981). For unknown reasons this method did not work well with COS-7 cells (even after appropriate modifications), although peroxisomal catalase was present as indicated by immunofluorescence. Therefore, we performed the ultrastructural studies with HepG2 cells, which exhibited similar morphological changes of peroxisomes as COS-7 cells after silencing of DLP1, and have been used for DAB cytochemistry before (Schrader et al., 1994). As shown in Fig. 2, consistent with light microscopy, HepG2 control cells contained predominantly spherical peroxisomes with variation in size and intensity of the DAB reaction. In cells silenced for DLP1, we frequently observed elongated peroxisomes. The elongated peroxisomes often had a segmented appearance, resembling beads on a string, but were still connected to each other (Fig. 2B,C). It is probable that these are peroxisomes caught actively during the fission process, which depends on DLP1. However, DLP1 function is obviously not required for the constriction of the peroxisomal membrane prior to fission. Electron-dense material or a cytoplasmic coat was not observed at the constriction sites.

To confirm that peroxisomal constriction can occur independently of DLP1, and that DLP1 is not associated with segmented peroxisomes under reduced DLP1 protein levels, we performed double-labeling experiments with anti-DLP1 antibodies in COS-7 cells expressing GFP-PTS1. As shown in Fig. 3, DLP1 was hardly detectable after siRNA treatment in those cells that contained elongated, segmented peroxisomes. The remaining DLP1 localized to a few small spots in the cytoplasm, but was not associated with the constriction sites on elongated

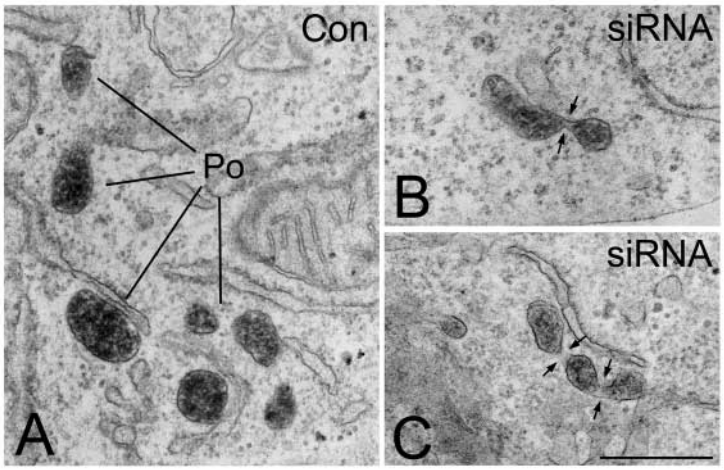


**Fig. 2.** Ultrastructure of peroxisomes in (A) controls and (B,C) after silencing of DLP1. HepG2 cells were transfected with buffer (Con) (A) or with DLP1 siRNA duplexes (B,C). After 48 hours the cells were processed for cytochemical visualization of peroxisomal catalase and embedded for electron microscopy. (A) Typical single, spherical peroxisomes (Po). (B,C) Peroxisomes after silencing of DLP1. They are arranged like beads on a string and are constricted but still interconnected (arrows). Bars, 500 nm.

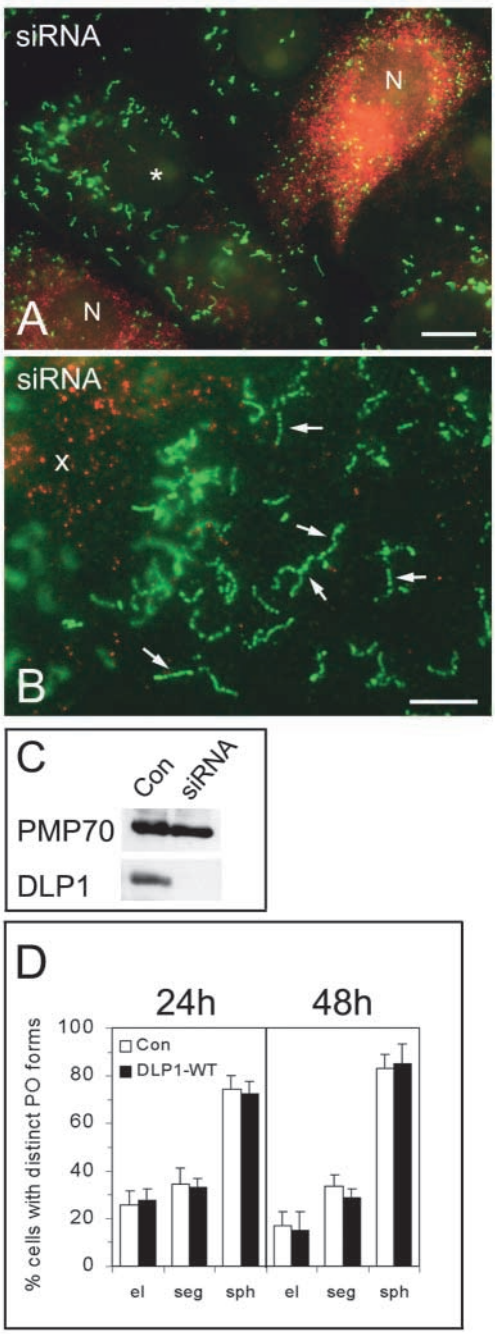


**Fig. 3.** Peroxisomal constriction can occur independently of DLP1. COS-7 cells stably expressing GFP-PTS1 were transfected with DLP1 siRNA duplexes (siRNA) and processed for immunofluorescence with anti-DLP1 antibodies 48 hours post transfection. (A,B) Co-localization of peroxisomes (green) and DLP1 (red). (A) DLP1 is efficiently silenced in cells that took up the DLP1 siRNA (asterisks). In those cells the remaining DLP1 localizes to a few small spots in the cytoplasm but is not associated with the constriction sites on elongated peroxisomes. Note the untransfected, non-silenced cell on the right, which has a high DLP1 protein level and contains spherical instead of elongated, segmented peroxisomes. (B) Higher magnification view of elongated, segmented peroxisomes (arrows) after efficient silencing of DLP1. Note the absence of co-localization of the remaining DLP1 with constricted peroxisomes. DLP1 is not efficiently silenced in the cell on the left (x). N, nucleus. (C) Immunoblots of peroxisomal fractions isolated from controls treated with buffer (Con) and cells transfected with DLP1 siRNA using anti-PMP70 and anti-DLP1 antibodies. Equal amounts of protein (PMP70, 10 μg/lane; DLP1, 45 μg/lane) were loaded onto the gels. Anti-PMP70 was used as a marker for peroxisomes. (D) Quantitation of peroxisome morphology at different times after transfection with a DLP1-WT construct. Cells were immunostained 24 and 48 hours after transfection by electroporation with antibodies to DLP1, and quantified. The data are from four independent experiments and are expressed as means ± s.d. Con, control cells (untransfected and vector only). For quantitative evaluation, cells were categorized as having elongated (el) (% of total), segmented (seg) (% of cells with elongated peroxisomes) or spherical (sph) (% of total) peroxisomes. Bars, 10 μm.

peroxisomes. Adjacent cells, which were presumably not or not sufficiently transfected with the DLP1 siRNA (about 15-20%), exhibited high levels of DLP1 and contained spherical but no elongated, segmented peroxisomes. These observations demonstrate that the DLP1 protein level in those cells that took up the DLP1 siRNA is much lower than indicated by the immunoblots performed with total cell homogenate (see Fig. 1G).

To further exclude an association of the remaining DLP1 protein with elongated peroxisomes after DLP1 silencing, peroxisomes were isolated from controls and silenced cells. Immunoblots with anti-DLP1 antibodies revealed no detectable association of the remaining DLP1 with the peroxisomal fraction isolated from silenced cells, whereas in control cells DLP1 was found to be associated with this fraction (Fig. 3C).

To examine the effect of high levels of DLP1 on peroxisomal elongation, constriction and fission, COS-7 cells expressing GFP-PTS1 were transfected with a DLP1-WT construct and processed for indirect immunofluorescence with anti-DLP1 antibodies after 24 and 48 hours. Quantification of the peroxisomal forms in those cells overexpressing DLP1 revealed no significant differences when compared to the appropriate controls (untransfected cells or vector only; Fig. 3D). Neither the frequency of cells with tubular or constricted peroxisomes nor the number of cells with small, spherical peroxisomes (produced by fission) was increased when the expression of DLP1 was elevated. Although DLP1 is known to function as a peroxisomal (and mitochondrial) fission enzyme, overexpression of DLP1 does obviously not increase peroxisomal fission, indicating that other proteins/factors are required in the peroxisomal fission process. Similar results were obtained with a DLP1-WT-GFP construct when expressed in COS-7 cells (not shown).

Taken together, these data clearly demonstrate that DLP1 is not directly involved in peroxisomal constriction, and that constriction can occur independently of DLP1 function.

## Pex11p functions in membrane enlargement of peroxisomes rather than in membrane division

The peroxisomal membrane protein Pex11pβ has been proposed to control peroxisome proliferation, and to function in the regulation of peroxisome size and number in mammalian cells (Schrader et al., 1998b; Li et al., 2002). When overexpressed, Pex11pβ induces a pronounced peroxisome

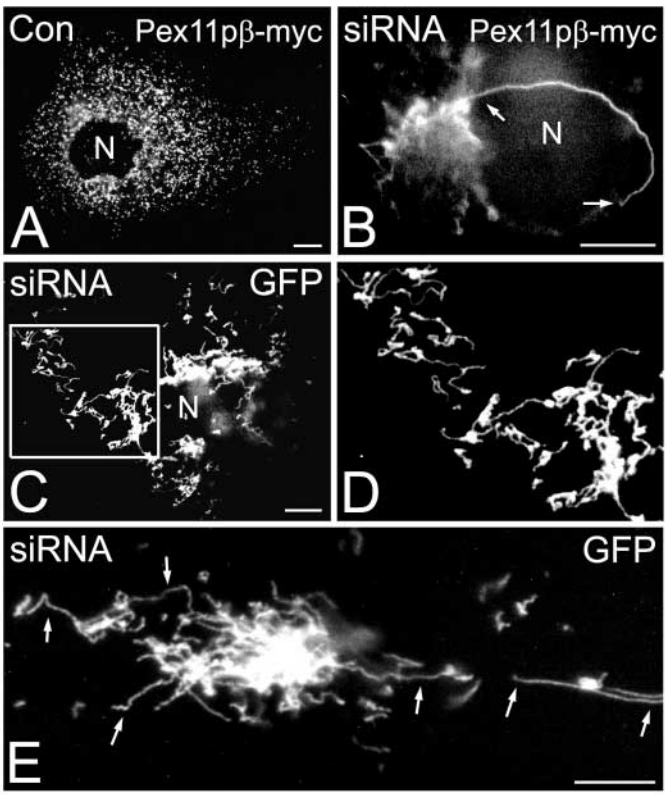


**Fig. 4.** Perturbation of peroxisome morphology by Pex11pβ expression after silencing of DLP1. COS-7 cells stably expressing GFP-PTS1 (GFP) were transfected with (A) buffer (Con) or (B-E) DLP1 siRNA duplexes (siRNA), incubated for 24 hours, transfected with a Pex11pβ-myc expression vector and another dose of siRNA duplexes, and processed for immunofluorescence after an additional 24 hours. (A,B) Pex11pβ-myc staining with antibodies to the myc epitope tag. (C-E) GFP-PTS1 labeling of peroxisomes in Pex11pβ-myc-expressing cells. (D) Higher magnification image of boxed region in C. Note the extreme tubulation of peroxisomes (arrows) in cells treated with DLP1 siRNA/Pex11pβ-myc, and the absence of peroxisome segmentation. N, nucleus. Bars, 10 μm.

proliferation through a multistep process involving peroxisome elongation and subsequent division (Schrader et al., 1998b). To examine its effect on peroxisome morphology and division in the absence of DLP1, we reduced DLP1 in COS-7 cells stably expressing GFP-PTS1 with DLP1 siRNA duplexes and transfected the cells with a Pex11pβ-myc expression vector to induce peroxisome proliferation. Cells were afterwards processed for indirect immunofluorescence using anti-myc antibodies. In control cells expressing Pex11pβ-myc, the formation of elongated peroxisomes and their subsequent separation into small, spherical organelles was observed (Fig. 4A). In cells silenced for DLP1, Pex11pβ-myc expression induced an extreme elongation of the peroxisomal compartment (Fig. 4B-E). This extensive elongation was even more pronounced than the one induced by silencing of DLP1 alone (compare Figs 1, 3 and 4). Furthermore, the formation of tubuloreticular networks of peroxisomes was observed (Fig. 4C,D). In some cells the elongated peroxisomes were found to cluster in a juxtanuclear region and to emanate tubular extensions from this complex tubuloreticular cluster (Fig. 4B,E). Single peroxisomal tubules up to 40 μm in length were frequently observed (Fig. 4B). In contrast to controls, division into small, spherical peroxisomes was completely inhibited. Furthermore, the constriction/segmentation of the elongated peroxisomes, which was observed after silencing of DLP1, was lost after expression of Pex11pβ (compare Figs 1, 3 and 4). These findings indicate that Pex11pβ is mainly involved in the process of growth and enlargement of the peroxisomal compartment.

## Silencing of DLP1 influences the morphology of specific membrane organelles in COS-7 cells

To further define the role of DLP1 in mammalian cells, we used DLP1 silencing to perturb DLP1 function, and evaluated the effects on other intracellular membrane organelles. COS-7 cells, which stably expressed GFP-PTS1, were transfected with buffer (or luciferase siRNA) or with DLP1 siRNA duplexes and processed for indirect immunofluorescence (Fig. 5). The prominent elongation of the peroxisomal compartment was used as a morphological indicator for efficient silencing of DLP1 in individual cells (Fig. 5A,C). In control cells, the Golgi membrane protein p115 was distributed in a compact juxtanuclear region in 70±3.8% of the cells (30% of the cells had a more dispersed, tubular Golgi morphology) (Fig. 5B). Silencing of DLP1 rendered the Golgi complex less compact, and the accumulation in the juxtanuclear region was partially lost. In addition, more elongated, tubular Golgi structures became visible (Fig. 5D). These alterations were observed in 76±3.8% of the cells silenced for DLP1. Similar results were obtained with an antibody to TGN38 (not shown). Furthermore, in control cells a co-localization of p115 and a DLP1-specific antibody was observed (Fig. 5E,F). The intensity of the DLP1 staining of the Golgi complex showed some variation among the cells. To examine the morphology of the Golgi structures in silenced COS-7 cells more closely, electron microscopy was performed. As shown in Fig. 6, control cells had normal Golgi structures with a modest concentration of Golgi stacks in the perinuclear area. COS-7 cells silenced for DLP1 possessed many clusters of Golgi stacks that were composed of tubulated cisternae and an extensive array of associated tubules and vesicles, which were spread in the perinuclear area.

For the labeling of the endoplasmic reticulum, COS-7 cells were transfected with a glycoprotein of the Marburg virus (MbVGP) (Becker et al., 1996). Prominent labeling of the nuclear envelope and ER tubules was observed in controls and in cells silenced for DLP1 (Fig. 5G-J). Based on our immunofluorescence studies, there were no striking differences in ER morphology between silenced cells and controls. This was also the case when the cells were transfected with the secretory protein ZG16p (Cronshagen et al., 1994), or after staining of the ER with an antibody to protein disulfide isomerase, as well as after labeling with the ER-specific fluorescent lectin concanavalin A (not shown).

Since DLP1 has been found localized to mitochondria and is suggested to function in the maintenance of mitochondrial morphology (Smirnova et al., 1998; Pitts et al., 1999), we also examined, as a positive control, the effect of a reduced DLP1 protein level on mitochondrial morphology. In control cells, mitochondria had either a tubular (9±4.5%) or globular

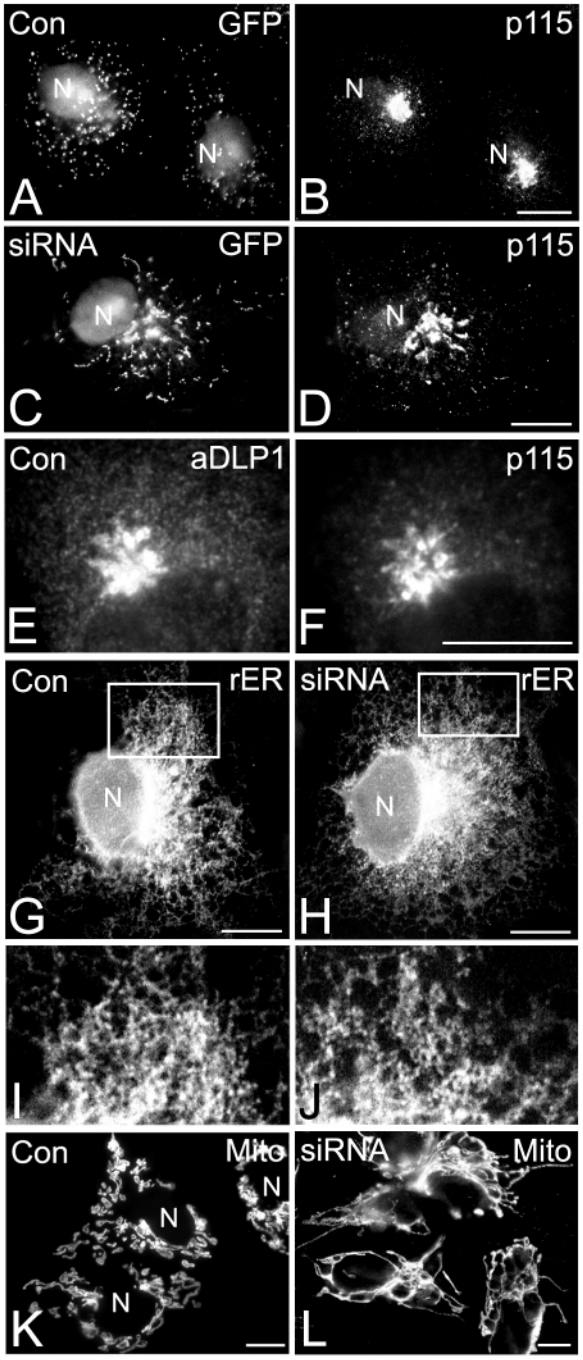


**Fig. 5.** Effects of DLP1 silencing on the morphology of other intracellular organelles in COS-7 cells. COS-7 cells stably expressing GFP-PTS1 were transfected with buffer (Con) (A,B,E,G,I,K) or with DLP1 siRNA duplexes (siRNA) (C,D,H,J,L) and processed for immunofluorescence 48 hours after the first transfection. (A,C) Visualization of peroxisomes by GFP-PTS1 (GFP). (B,D) Golgi staining with anti-p115 antibodies. (E, F) Co-localization of DLP1 and p115 in untransfected COS-7 cells (not expressing GFP-PTS1). For rER labeling (G-J) cells were transfected with DLP1 siRNA duplexes, incubated for 24 hours, transfected with a Marburg virus glycoprotein (MbVGP) expression vector and another dose of siRNA duplexes, and processed after an additional 24 hours. Cells were incubated with anti-MbVGP antibodies. (I,J) Higher magnification images of boxed regions in G,H. (K,L) Staining of mitochondria with antibodies to MnSOD. Note the largely elongated peroxisomes (C) and mitochondria (L) after silencing of DLP1 compared to the appropriate controls. N, nucleus. Bars, 10 μm.

(91±3.5%) morphology (Fig. 5K). Thick tubules and bulbous mitochondrial structures were frequently observed. After silencing of DLP1, mitochondria became highly elongated and formed thin tubules as well as prominent tubuloreticular networks in 80±3.8% of the silenced cells (Fig. 5L). These observations indicate that mitochondrial fission is inhibited in the absence of DLP1, and that the balance between fusion and fission is shifted towards mitochondrial fusion.

When lysosomes were stained with an antibody to the lysosomal membrane protein lamp1, no clear morphological changes of this endocytic organelle were found in controls and in DLP1-silenced cells (not shown). Furthermore, we observed no effects of DLP1 silencing on the organization of the microtubule system (see Fig. 7A,B).

Taken together, these results show that the effects of DLP1 silencing are specific for a subset of membrane organelles that in COS-7 cells includes mitochondria, peroxisomes and the Golgi complex. A common feature of the morphological changes of these organelles is a shift towards more elongated membranes, which is likely to be caused by a loss of DLP1 and its proposed function in membrane fission.

### Microtubule-dependent dynamics of elongated peroxisomes after silencing of DLP1

It has become evident from in vivo studies in the last few years that the peroxisomal compartment is more complex and dynamic than previously expected (Schrader et al., 2003). Mammalian peroxisomes interact with and move along microtubules to guarantee a uniform intracellular distribution (Schrader et al., 1996; Rapp et al., 1996; Wiemer et al., 1997), whereas peroxisomes in yeast and plant cells move along the actin cytoskeleton (Hoepfner et al., 2001; Mathur et al., 2002). Since the function and dynamic behavior of more complex peroxisomal structures is less well understood, we took advantage of our initial observation, that silencing of DLP1 induces the formation of elongated, tubular peroxisomes in a high proportion (70-80%) of DLP1 siRNA-treated cells. To examine the dynamic behavior of those elongated peroxisomes, we transfected COS-7 cells stably expressing GFP-PTS1 with DLP1 siRNA duplexes and processed them for immunofluorescence or live cell imaging studies (Fig. 7). As shown in Fig. 7A,B, we observed no effects of DLP1 silencing on the organization of microtubules in COS-7 cells. The microtubules in controls and silenced cells had normal radial microtubule arrays which were clearly focused at the centrosome. No changes were observed in the sensitivity to nocodazole-induced microtubule depolymerization, or in the rate of centrosome-based microtubule regrowth after nocodazole washout (not shown). After nocodazole treatment of cells silenced for DLP1 no collapse or fragmentation of elongated peroxisomes was observed (Fig. 7C,D,G). However, the uniform intracellular distribution of peroxisomes was

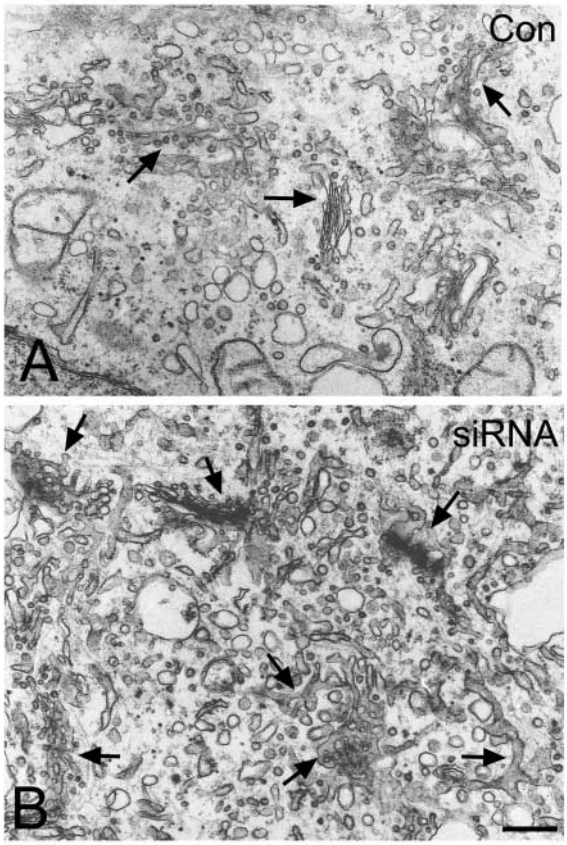


**Fig. 6.** Ultrastructure of the Golgi complex in (A) controls and (B) after silencing of DLP1. COS-7 cells were transfected with buffer (Con) (A) or with DLP1 siRNA duplexes (B). Cells were fixed and prepared for electron microscopy 48 hours post transfection. (A) Control cell with a modest concentration of Golgi stacks (arrows). (B) Cells silenced for DLP1 display many clusters of Golgi stacks. Classic cisternae and an extensive array of associated tubules and vesicles are visible (arrows). Bar, 500 nm.

disturbed, and small aggregates of peroxisomes were formed as a result of an inhibition of peroxisomal motility (Fig. 7C). These findings are consistent with earlier observations on the effects of microtubule-active drugs on peroxisome morphology and distribution in untreated cells (Schrader et al., 1996). Next we analyzed the dynamic properties of elongated peroxisomes in living cells silenced for DLP1 by time-lapse microscopy (Fig. 7E-F). A subset of the elongated peroxisomes (approx. 10-15%; especially smaller ones measuring up to 5 μm in length) exhibited fast, directional movements along linear or curved trajectories (approx. 0.6±0.3 μm/second) (Fig. 7E). These movements were completely inhibited by nocodazole (Fig. 7G) indicating that they were microtubule dependent. The elongated peroxisomes were observed to move over relatively long distances (range: 1.5-12 μm, mean: 3.5±1.5 μm). Highly elongated peroxisomes (more than 5-10 μm in length) showed little net displacement. Actually, the majority of the elongated peroxisomes (approx. 85-90%) exhibited short-range, non-directed, oscillatory movements, which continued after depolymerization of microtubules and are likely to represent Brownian motion. Interestingly, elongated peroxisomes in cells silenced for DLP1 were often observed to emanate tubular projections, which appeared to interact with other peroxisomal structures before they were retracted (Fig. 7F). The formation and directed movement of the tubular projections was also inhibited by nocodazole. Owing to the low half-life of elongated peroxisomes in normal cells, this kind of microtubule-dependent peroxisomal interaction has not been observed before, and emphasizes that peroxisomes are more dynamic and interactive than previously assumed.

## Discussion

Until recently, little information was available on the mechanisms and factors involved in the growth and division of the peroxisomal compartment in mammalian cells. Now, our knowledge about proteins required for peroxisomal division is slowly increasing (Fig. 8). In this study we extended our previous observation that DLP1, a dynamin-like protein of mammals, plays a critical role in peroxisome division, and demonstrate that silencing of DLP1 offers the promise of a powerful new means of addressing DLP1 function in mammalian cells.

### Elongation of peroxisomes – a prerequisite for division

Elongated, tubular peroxisomes have been described in several mammalian tissues and cell lines, but their exact function remained unclear (Hicks and Fahimi, 1977; Gorgas, 1984; Yamamoto and Fahimi, 1987; Roels et al., 1991). Since tubular peroxisomes were frequently observed under conditions of rapid cellular growth (Yamamoto and Fahimi, 1987) or after stimulation of cultured cells with growth factors, fatty acids or free radicals (Schrader et al., 1998a; Schrader et al., 1999), they have been proposed to contribute to peroxisome proliferation. A striking observation of our immunofluorescence experiments was the pronounced formation of elongated peroxisomes (in 70-80% of the cells) induced solely by a reduction of DLP1 through siRNA in the absence of any additional proliferative stimuli. These findings indicate that the elongation process of peroxisomes can occur without DLP1 and precedes peroxisomal fission. They further imply that peroxisome elongation is a permanent, constitutive process. Once fission is blocked, elongated peroxisomes start to accumulate. The extent of peroxisome elongation may vary depending on the 'proliferative capacity' of peroxisomes which in turn is influenced by the metabolic requirements of different cell lines, tissues and species.

A significant but modest elongation of peroxisomes was observed in our recent study, when a dominant-negative mutant of DLP1 (K38A) defective in GTP hydrolysis was expressed (Koch et al., 2003), indicating that both methods, silencing of DLP1 and expression of a dominant-negative mutant, exert slightly different effects on the peroxisomal compartment. A pronounced elongation of peroxisomes was only observed, when DLP1-K38A was co-expressed with Pex11pβ, a peroxisomal membrane protein known to stimulate peroxisome proliferation in a multistep process. Interestingly, the first step induced by Pex11pβ is peroxisome elongation, followed by segregation of peroxisomal proteins and subsequent division (Schrader et al., 1998b). A striking increase in elongated peroxisomal forms on expression of Pex11p has been observed in all organisms studied including yeast, trypanosomes and

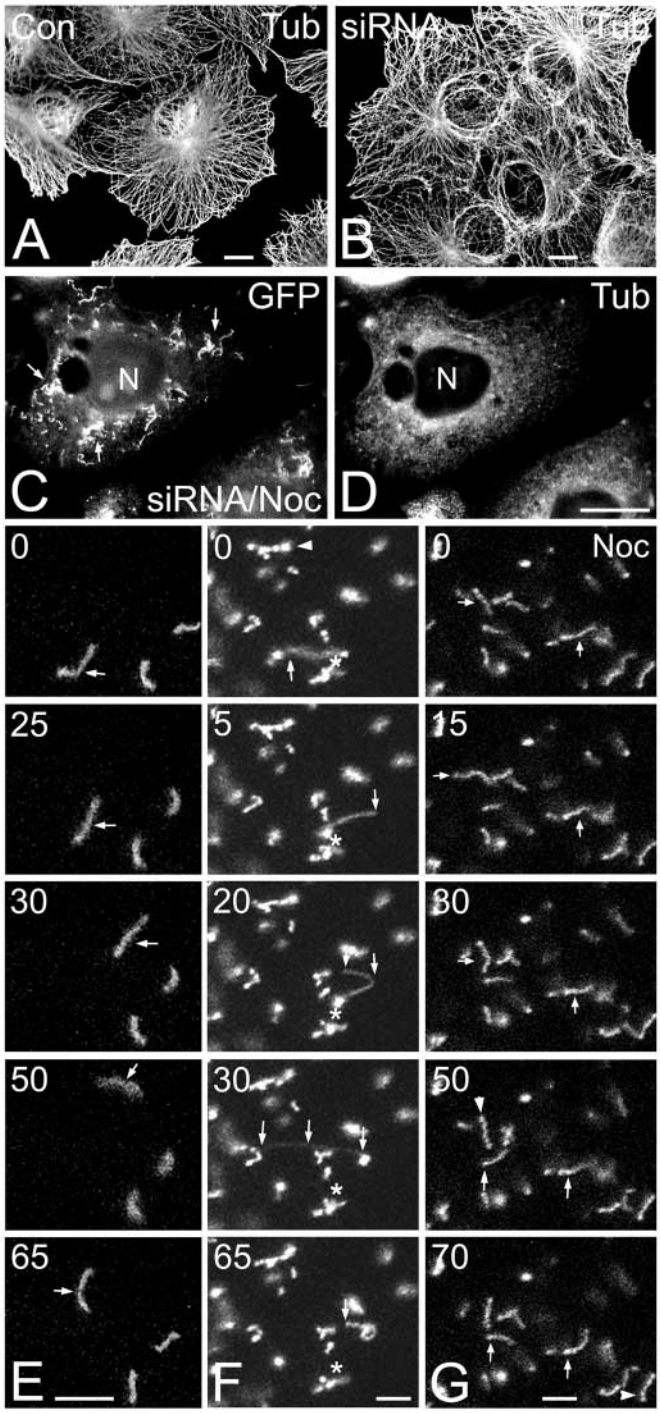


**Fig. 7.** Influence of the microtubule cytoskeleton on peroxisomal morphology and dynamics after silencing of DLP1. COS-7 cells stably expressing GFP-PTS1 (GFP) were transfected with (A) buffer (Con) or (B-G) DLP1 siRNA duplexes (siRNA) and processed for immunofluorescence (A-D) or live-cell imaging (E-G). Cells in C,D,G were treated with nocodazole to depolymerize microtubules. (A,B,D) Immunofluorescence of COS-7 cells using antibodies to tubulin (Tub). (C) Visualization of peroxisomes labeled with GFP-PTS1 after transfection with DLP1 siRNA and treatment with nocodazole. Arrows point to peroxisomal aggregates. (E-G) Images of the motile behavior of individual, elongated peroxisomes *in vivo* after silencing of DLP1. Numbers in the top right of the panels show time elapsed in seconds. In E, an elongated peroxisome (arrow) moves to the right of the image (0 to 30 seconds) before it continues to move on a circular track (50 to 65 seconds). In F, an elongated peroxisome (arrows) with a globular structure at one end (*) moves from the left to the right of the image (0 to 5 seconds). Afterwards it emanates a tubular projection and moves to the left of the image (30 seconds), presumably to interact with another peroxisome, before it retracts and collapses into a circular structure (65 seconds). In G, the dynamic behavior of elongated peroxisomes after depolymerization of microtubules with nocodazole is shown. Arrows mark the positions of elongated peroxisomes and arrowheads point to segmented organelles. N, nucleus. Bars, 10 μm (A-D), 5 μm (E-G).

mammalian cells, further indicating that peroxisome tubule formation is a prerequisite for peroxisome division (Erdmann and Blobel, 1995; Schrader et al., 1996; Schrader et al., 1998b; Lorenz et al., 1998).

### DLP1 divides, but does not constrict peroxisomes

A division of the elongated, tubular peroxisomes into spherical organelles was completely inhibited after the loss of DLP1 function, either by silencing (Fig. 1) or expression of a non-functional mutant (Koch et al., 2003), as indicated by our quantitative analyses. The peroxisomal phenotypic changes found in COS-7 and other cells therefore confirm a direct function of DLP1 in peroxisomal fission. In addition, our immunofluorescence and ultrastructural studies now reveal that DLP1 is obviously not directly involved in peroxisomal constriction. Our findings demonstrate that membrane constriction can occur in the absence of DLP1, and indicate that additional peroxisomal (membrane) proteins are required for this process (Fig. 8). Since a peroxisomal tubule has an average diameter of approx. 100±20 nm, constriction may cause a thinning of the membrane tubule to favor the association of DLP1 (and additional factors) around the tube. It is therefore probable that constriction of the peroxisomal membrane takes place before DLP1 recruitment, which is then followed by subsequent peroxisomal fission. A similar view has been favored for mitochondria: it has been suggested that mitochondrial constriction and fission in *S. cerevisiae* require distinct sets of molecular components, and that the dynamin-related protein Dnm1p functions primarily or exclusively in the latter process (Legesse-Miller et al., 2003). Recently, Mdm33, a component which might be involved in mitochondrial constriction in *S. cerevisiae*, has been identified by Messerschmitt et al. (Messerschmitt et al., 2003). Furthermore, mitochondrial structures that resemble the peroxisomal 'beads on a string' have been observed in *C. elegans* DRP-1 mutants (Labrousse et al., 1999).

### Pex11pβ does neither constrict nor divide peroxisomes

Pex11pβ has been implicated in the regulation of peroxisome size, number and division. We now show that expression of Pex11pβ in addition to silencing of DLP1 results in an extreme elongation of peroxisomes (up to 40 μm in length) which was even more pronounced than the one induced by silencing of DLP1 alone or by co-expression of the dominant-negative mutant DLP1-K38A (Koch et al., 2003), and in the formation of large tubuloreticular networks of peroxisomes. These

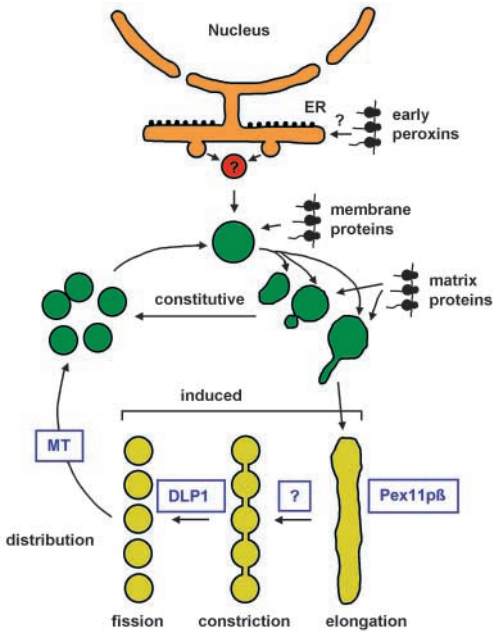


**Fig. 8.** Schematic model for the morphogenesis of mammalian peroxisomes, based on observations reported here and previously (Schrader et al., 1996; Schrader et al., 1998b; Schrader et al., 2000). Recent evidence suggesting the involvement of the ER in the de novo formation of peroxisomes (Titorenko and Rachubinski, 2001; Eckert and Erdmann, 2003; Lazarow, 2003) is included. The majority of matrix and membrane proteins are synthesized on free ribosomes in the cytosol and imported post-translationally into pre-existing peroxisomes. Peroxisomes multiply by budding and segmentation from pre-existing ones. Under induced conditions (e.g. cultures at low density, growth factors, fatty acids, free radicals), highly elongated peroxisomes are formed that undergo segmentation and fission, forming spherical peroxisomes. Pex11pβ is involved in the elongation/tubulation of peroxisomes (Schrader et al., 1998b), whereas DLP1 mediates peroxisomal fission (Koch et al., 2003; Li and Gould, 2003). Proteins mediating the constriction of peroxisomes are presently unknown. Proper intracellular distribution of the formed peroxisomes requires microtubules and a functional dynein/dynactin motor (Schrader et al., 2003). In yeast and plants peroxisomes are distributed via the actin cytoskeleton (Hoepfner et al., 2001; Mathur et al., 2002).

findings indicate that Pex11pβ is still able to induce growth and enlargement of the peroxisomal compartment in the absence of DLP1, but is itself not capable of dividing or constricting peroxisomal membranes. Interestingly, the peroxisomal constriction observed after silencing of DLP1 was absent from Pex11pβ-induced peroxisomal tubules. It is probable that Pex11pβ expression modifies the peroxisomal membrane and alters the assembly of the constriction factors. We therefore propose a major function for Pex11pβ in the enlargement and modification of the peroxisomal membrane prior to division rather than in the fission process itself (Fig. 8). The similarities of the yeast Pex11p with the ligand-binding domain of nuclear hormone receptors might point to a role in phospholipid-binding (Barnett et al., 2000). This might result in the modification of the peroxisomal membrane, and subsequently in its elongation. Although a direct interaction between DLP1 and Pex11p has not been detected (Li and Gould, 2003), the membrane modifying activity of Pex11p might support the recruitment of the fission machinery to peroxisomes through an indirect mechanism.

The Pex11p-induced network formation of peroxisomes is likely to result from a shift in the balance between fission and fusion of peroxisomes. It has recently been shown that peroxisomes are more dynamic and interactive than previously assumed. For example, interconnecting and separating tubular peroxisomes forming a reticulum have been observed by real time imaging (Schrader et al., 2000). The enrichment of elongated peroxisomes through silencing of DLP1 has now offered an opportunity to analyze their dynamic behavior and their motile properties in more detail. Interestingly, those peroxisomes moved in a microtubule-dependent manner, and were often observed to emanate tubular projections, which appeared to interact with other peroxisomal structures before they were retracted. These findings further emphasize the importance of the microtubular system for peroxisome dynamics in mammalian cells (Fig. 8), and are indicative of the presence of a putative fusion machinery on peroxisomal membranes.

## DLP1 acts on several membranous organelles

DLP1 forms a homotetrameric complex similar to dynamin (Shin et al., 1999) and has been demonstrated to form rings and tubulate membranes in a nucleotide-dependent manner both in living cells and in vitro (Yoon et al., 2001). However, the importance of mammalian DLP1 for different membranous organelles is a matter of considerable controversy. It has been reported to be localized to the perinuclear region (Imoto et al., 1998), to cytoplasmic vesicles and tubules of the endoplasmic reticulum (Yoon et al., 1998), to mitochondria (Smirnova et al., 1998; Pitts et al., 1999) and recently to peroxisomes (Koch et al., 2003; Li and Gould, 2003). Based on studies with a mutant DLP1 (K38A), a major function in the maintenance of mitochondrial morphology had been suggested, whereas a role in maintenance of other intracellular organelles including peroxisomes was excluded (Smirnova et al., 1998). Using DLP1 siRNA, we can now confirm a major function for DLP1 in the maintenance of mitochondrial as well as peroxisomal morphology and division. However, we also observed an effect on the Golgi complex, which exhibited an enlarged and more tubular morphology in COS-7 cells. Ultrastructural studies revealed many clusters of Golgi stacks that were composed of classic cisternae and an extensive array of associated tubules and vesicles. This observation was facilitated by the usually compact and well focussed Golgi structures in COS-7 cells, and is unlikely to result from indirect effects on the organization of the cytoskeleton. Similar to its modest effect on peroxisomes, the expression of DLP1-K38A might exert only a weak effect on Golgi morphology when compared to DLP1 silencing, which can be easily overlooked. However, whereas the Golgi complex in COS-7 cells could be stained with a DLP1-specific antibody, staining was absent in some other cell lines tested (M.S., unpublished). This finding might either point to the presence of distinct DLP1 isoforms, which are expressed in a tissue-specific manner (McNiven et al., 2000) or to differences in the recruitment of cytosolic DLP1 to organelle membranes. In support of the latter assumption, recruitment of DLP1 to peroxisomes was significantly increased after the stimulation of peroxisome proliferation

(Koch et al., 2003). The specific expression of distinct DLP1 isoforms and differences in DLP1 recruitment might also explain why silencing of DLP1 had no visible effect on the endoplasmic reticulum in COS-7 cells, whereas in other cells morphological changes were observed after perturbance of DLP1 function (Yoon et al., 1998). In summary, these results demonstrate that DLP1 acts on multiple membranous organelles, and emphasize that it is part of a general fission machinery used by distinct organelles. Silencing of DLP1 by siRNA appears to be a general, effective tool for blocking DLP1 function in the cell, and should be of considerable value in future physiological and mechanistic studies.

The authors are grateful to M. A. McNiven (Mayo Clinic, Rochester, USA), H. D. Söling (Max-Planck-Institute of Biophysical Chemistry, Göttingen, Germany), A. Völkl (University of Heidelberg, Germany), M. Eilers and S. Becker (University of Marburg, Germany) for providing antibodies and cDNA constructs. We thank B. Agricola and W. Ackermann (Marburg, Germany) for excellent technical assistance, and V. Kramer (Marburg, Germany) for help with the photographic work and image processing. This work was partially supported by a grant of the Medizin Stiftung, Marburg, Germany (to A.K.).

## References

**Angermuller, S. and Fahimi, H. D.** (1981). Selective cytochemical localization of peroxidase, cytochrome oxidase and catalase in rat liver with 3,3′-diaminobenzidine. *Histochemistry* **71**, 33-44.

**Barnett, P., Tabak, H. F. and Hettema, E. H.** (2000). Nuclear receptors arose from pre-existing protein modules during evolution. *Trends Biochem. Sci.* **25**, 227-228.

**Becker, S., Klenk, H. D. and Muhlberger, E.** (1996). Intracellular transport and processing of the Marburg virus surface protein in vertebrate and insect cells. *Virology* **225**, 145-155.

**Chang, C. C., South, S., Warren, D., Jones, J., Moser, A. B., Moser, H. W. and Gould, S. J.** (1999). Metabolic control of peroxisome abundance. *J. Cell Sci.* **112**, 1579-1590.

**Cronshagen, U., Voland, P. and Kern, H. F.** (1994). cDNA cloning and characterization of a novel 16 kDa protein located in zymogen granules of rat pancreas and goblet cells of the gut. *Eur. J. Cell Biol.* **65**, 366-377.

**Danino, D. and Hinshaw, J. E.** (2001). Dynamin family of mechanoenzymes. *Curr. Opin. Cell Biol.* **13**, 454-460.

**Eckert, J. H. and Erdmann, R.** (2003). Peroxisome biogenesis. *Rev. Physiol. Biochem. Pharmacol.* **147**, 75-121.

**Elbashir, S. M., Harborth, J., Lendeckel, W., Yalcin, A., Weber, K. and Tuschl, T.** (2001). Duplexes of 21-nucleotide RNAs mediate RNA interference in cultured mammalian cells. *Nature* **411**, 494-498.

**Erdmann, R. and Blobel, G.** (1995). Giant peroxisomes in oleic acid-induced *Saccharomyces cerevisiae* lacking the peroxisomal membrane protein Pmp27p. *J. Cell Biol.* **128**, 509-523.

**Faber, K. N., Haan, G. J., Baerends, R. J., Kram, A. M. and Veenhuis, M.** (2002). Normal peroxisome development from vesicles induced by truncated Hansenula polymorpha Pex3p. *J. Biol. Chem.* **277**, 11026-11033.

**Fischer, D., Bieber, T., Li, Y., Elsasser, H. P. and Kissel, T.** (1999). A novel non-viral vector for DNA delivery based on low molecular weight, branched polyethylenimine: effect of molecular weight on transfection efficiency and cytotoxicity. *Pharm. Res.* **16**, 1273-1279.

**Geuze, H. J., Murk, J. L., Stroobants, A. K., Griffith, J. M., Kleijmeer, M. J., Koster, A. J., Verkleij, A. J., Distel, B. and Tabak, H. F.** (2003). Involvement of the endoplasmic reticulum in peroxisome formation. *Mol. Biol. Cell* **14**, 2900-2907.

**Gorgas, K.** (1984). Peroxisomes in sebaceous glands. V. Complex peroxisomes in the mouse preputial gland: serial sectioning and three-dimensional reconstruction studies. *Anat. Embryol. (Berl.)* **169**, 261-270.

**Hicks, L. and Fahimi, H. D.** (1977). Peroxisomes (microbodies) in the myocardium of rodents and primates. A comparative ultrastructural cytochemical study. *Cell Tissue Res.* **175**, 467-481.

**Hoepfner, D., van den Berg, M., Philippsen, P., Tabak, H. F. and Hettema, E. H.** (2001). A role for Vps1p, actin, and the Myo2p motor in peroxisome abundance and inheritance in *Saccharomyces cerevisiae*. *J. Cell Biol.* **155**, 979-990.

**Imoto, M., Tachibana, I. and Urrutia, R.** (1998). Identification and functional characterization of a novel human protein highly related to the yeast dynamin-like GTPase Vps1p. *J. Cell Sci.* **111**, 1341-1349.

**Koch, A., Thiemann, M., Grabenbauer, M., Yoon, Y., McNiven, M. A. and Schrader, M.** (2003). Dynamin-like protein 1 is involved in peroxisomal fission. *J. Biol. Chem.* **278**, 8597-8605.

**Labrousse, A. M., Zappaterra, M. D., Rube, D. A. and van der Bliek, A. M.** (1999). *C. elegans* dynamin-related protein DRP-1 controls severing of the mitochondrial outer membrane. *Mol. Cell* **4**, 815-826.

**Lazarow, P. B.** (2003). Peroxisome biogenesis: advances and conundrums. *Curr. Opin. Cell Biol.* **15**, 489-497.

**Lazarow, P. B. and Fujiki, Y.** (1985). Biogenesis of peroxisomes. *Annu. Rev. Cell Biol.* **1**, 489-530.

**Legesse-Miller, A., Massol, R. H. and Kirchhausen, T.** (2003). Constriction and Dnm1p recruitment are distinct processes in mitochondrial fission. *Mol. Biol. Cell* **14**, 1953-1963.

**Li, X. and Gould, S. J.** (2002). PEX11 promotes peroxisome division independently of peroxisome metabolism. *J. Cell Biol.* **156**, 643-651.

**Li, X. and Gould, S. J.** (2003). The dynamin-like GTPase DLP1 is essential for peroxisome division and is recruited to peroxisomes in part by PEX11. *J. Biol. Chem.* **278**, 17012-17020.

**Li, X., Baumgart, E., Morrell, J. C., Jimenez-Sanchez, G., Valle, D. and Gould, S. J.** (2002). PEX11 beta deficiency is lethal and impairs neuronal migration but does not abrogate peroxisome function. *Mol. Cell Biol.* **22**, 4358-4365.

**Lorenz, P., Maier, A. G., Baumgart, E., Erdmann, R. and Clayton, C.** (1998). Elongation and clustering of glycosomes in *Trypanosoma brucei* overexpressing the glycosomal Pex11p. *EMBO J.* **17**, 3542-3555.

**Luers, G., Hashimoto, T., Fahimi, H. D. and Volkl, A.** (1993). Biogenesis of peroxisomes: isolation and characterization of two distinct peroxisomal populations from normal and regenerating rat liver. *J. Cell Biol.* **121**, 1271-1280.

**Luers, G. H., Schad, A., Fahimi, H. D., Voelkl, A. and Seitz, J.** (2003). Expression of peroxisomal proteins provides clear evidence for the presence of peroxisomes in the male germ cell line GC1spg. *Cytogenet. Genome Res.* **103**, 360-365.

**Marshall, P. A., Krimkevich, Y. I., Lark, R. H., Dyer, J. M., Veenhuis, M. and Goodman, J. M.** (1995). Pmp27 promotes peroxisomal proliferation. *J. Cell Biol.* **129**, 345-355.

**Mathur, J., Mathur, N. and Hulskamp, M.** (2002). Simultaneous visualization of peroxisomes and cytoskeletal elements reveals actin and not microtubule-based peroxisome motility in plants. *Plant Physiol.* **128**, 1031-1045.

**McNiven, M. A.** (1998). Dynamin: a molecular motor with pinchase action. *Cell* **94**, 151-154.

**McNiven, M. A., Cao, H., Pitts, K. R. and Yoon, Y.** (2000). The dynamin family of mechanoenzymes: pinching in new places. *Trends Biochem. Sci.* **25**, 115-120.

**Messerschmitt, M., Jakobs, S., Vogel, F., Fritz, S., Dimmer, K. S., Neupert, W. and Westermann, B.** (2003). The inner membrane protein Mdm33 controls mitochondrial morphology in yeast. *J. Cell Biol.* **160**, 553-564.

**Passreiter, M., Anton, M., Lay, D., Frank, R., Harter, C., Wieland, F. T., Gorgas, K. and Just, W. W.** (1998). Peroxisome biogenesis: involvement of ARF and coatomer. *J. Cell Biol.* **141**, 373-383.

**Pitts, K. R., Yoon, Y., Krueger, E. W. and McNiven, M. A.** (1999). The dynamin-like protein DLP1 is essential for normal distribution and morphology of the endoplasmic reticulum and mitochondria in mammalian cells. *Mol. Biol. Cell* **10**, 4403-4417.

**Poll-The, B. T., Roels, F., Ogier, H., Scotto, J., Vamecq, J., Schutgens, R. B., Wanders, R. J., van Roermund, C. W., van Wijland, M. J., Schram, A. W. et al.** (1988). A new peroxisomal disorder with enlarged peroxisomes and a specific deficiency of acyl-CoA oxidase (pseudo-neonatal adrenoleukodystrophy). *Am. J. Hum. Genet.* **42**, 422-434.

**Rapp, S., Saffrich, R., Anton, M., Jakle, U., Ansorge, W., Gorgas, K. and Just, W. W.** (1996). Microtubule-based peroxisome movement. *J. Cell Sci.* **109**, 837-849.

**Roels, F., Espeel, M., Pauwels, M., de Craemer, D., Egberts, H. J. and van der Spek, P.** (1991). Different types of peroxisomes in human duodenal epithelium. *Gut* **32**, 858-865.

**Rottensteiner, H., Stein, K., Sonnenhol, E. and Erdmann, R.** (2003). Conserved function of pex11p and the novel pex25p and pex27p in peroxisome biogenesis. *Mol. Biol. Cell* **14**, 4316-4328.

**Sacksteder, K. A. and Gould, S. J.** (2000). The genetics of peroxisome biogenesis. *Annu. Rev. Genet.* **34**, 623-652.

**Sakai, Y., Marshall, P. A., Saiganji, A., Takabe, K., Saiki, H., Kato, N. and Goodman, J. M.** (1995). The Candida boidinii peroxisomal membrane protein Pmp30 has a role in peroxisomal proliferation and is functionally homologous to Pmp27 from *Saccharomyces cerevisiae*. *J. Bacteriol.* **177**, 6773-6781.

**Schrader, M., Baumgart, E., Volkl, A. and Fahimi, H. D.** (1994). Heterogeneity of peroxisomes in human hepatoblastoma cell line HepG2. Evidence of distinct subpopulations. *Eur. J. Cell Biol.* **64**, 281-294.

**Schrader, M., Burkhardt, J. K., Baumgart, E., Luers, G., Spring, H., Volkl, A. and Fahimi, H. D.** (1996). Interaction of microtubules with peroxisomes. Tubular and spherical peroxisomes in HepG2 cells and their alterations induced by microtubule-active drugs. *Eur. J. Cell Biol.* **69**, 24-35.

**Schrader, M., Krieglstein, K. and Fahimi, H. D.** (1998a). Tubular peroxisomes in HepG2 cells: selective induction by growth factors and arachidonic acid. *Eur. J. Cell Biol.* **75**, 87-96.

**Schrader, M., Reuber, B. E., Morrell, J. C., Jimenez-Sanchez, G., Obie, C., Stroh, T. A., Valle, D., Schroer, T. A. and Gould, S. J.** (1998b). Expression of PEX11beta mediates peroxisome proliferation in the absence of extracellular stimuli. *J. Biol. Chem.* **273**, 29607-29614.

**Schrader, M., Wodopia, R. and Fahimi, H. D.** (1999). Induction of tubular peroxisomes by UV irradiation and reactive oxygen species in HepG2 cells. *J. Histochem. Cytochem.* **47**, 1141-1148.

**Schrader, M., King, S. J., Stroh, T. A. and Schroer, T. A.** (2000). Real time imaging reveals a peroxisomal reticulum in living cells. *J. Cell Sci.* **113**, 3663-3671.

**Schrader, M., Thiemann, M. and Fahimi, H. D.** (2003). Peroxisomal motility and interaction with microtubules. *Microsc. Res. Tech.* **61**, 171-178.

**Shin, H. W., Takatsu, H., Mukai, H., Munekata, E., Murakami, K. and Nakayama, K.** (1999). Intermolecular and interdomain interactions of a dynamin-related GTP-binding protein, Dnm1p/Vps1p-like protein. *J. Biol. Chem.* **274**, 2780-2785.

**Smirnova, E., Shurland, D. L., Ryazantsev, S. N. and van der Bliek, A. M.** (1998). A human dynamin-related protein controls the distribution of mitochondria. *J. Cell Biol.* **143**, 351-358.

**Smirnova, E., Griparic, L., Shurland, D. L. and van der Bliek, A. M.** (2001). Dynamin-related protein Drp1 is required for mitochondrial division in mammalian cells. *Mol. Biol. Cell* **12**, 2245-2256.

**Smith, J. J., Marelli, M., Christmas, R. H., Vizeacoumar, F. J., Dilworth, D. J., Ideker, T., Galitski, T., Dimitrov, K., Rachubinski, R. A. and Aitchison, J. D.** (2002). Transcriptome profiling to identify genes involved in peroxisome assembly and function. *J. Cell Biol.* **158**, 259-271.

**South, S. T. and Gould, S. J.** (1999). Peroxisome synthesis in the absence of preexisting peroxisomes. *J. Cell Biol.* **144**, 255-266.

**Tam, Y. Y., Torres-Guzman, J. C., Vizeacoumar, F. J., Smith, J. J., Marelli, M., Aitchison, J. D. and Rachubinski, R. A.** (2003). Pex11-related proteins in peroxisome dynamics: a role for the novel peroxin Pex27p in controlling peroxisome size and number in *Saccharomyces cerevisiae*. *Mol. Biol. Cell* **14**, 4089-4102.

**Titorenko, V. I. and Rachubinski, R. A.** (2001). The life cycle of the peroxisome. *Nat. Rev. Mol. Cell Biol.* **2**, 357-368.

**van den Bosch, H., Schutgens, R. B., Wanders, R. J. and Tager, J. M.** (1992). Biochemistry of peroxisomes. *Annu. Rev. Biochem.* **61**, 157-197.

**van Roermund, C. W., Tabak, H. F., van den Berg, M., Wanders, R. J. and Hettema, E. H.** (2000). Pex11p plays a primary role in medium-chain fatty acid oxidation, a process that affects peroxisome number and size in *Saccharomyces cerevisiae*. *J. Cell Biol.* **150**, 489-498.

**Völkl, A., Baumgart, E. and Fahimi, H. D.** (1996). Isolation and characterization of peroxisomes. In *Subcellular Fractionation: A Practical Approach* (ed. J. Graham and D. Rickwood), pp. 143-167. Oxford, UK: Oxford University Press.

**Wiemer, E. A., Wenzel, T., Deerinck, T. J., Ellisman, M. H. and Subramani, S.** (1997). Visualization of the peroxisomal compartment in living mammalian cells: dynamic behavior and association with microtubules. *J. Cell Biol.* **136**, 71-80.

**Yamamoto, K. and Fahimi, H. D.** (1987). Three-dimensional reconstruction of a peroxisomal reticulum in regenerating rat liver: evidence of interconnections between heterogeneous segments. *J. Cell Biol.* **105**, 713-722.

**Yoon, Y., Pitts, K. R., Dahan, S. and McNiven, M. A.** (1998). A novel dynamin-like protein associates with cytoplasmic vesicles and tubules of the endoplasmic reticulum in mammalian cells. *J. Cell Biol.* **140**, 779-793.

**Yoon, Y., Pitts, K. R. and McNiven, M. A.** (2001). Mammalian dynamin-like protein DLP1 tubulates membranes. *Mol. Biol. Cell* **12**, 2894-2905.